

# Extrinsic Doping of Electrodeposited Zinc Oxide Films by Chlorine for Transparent Conductive Oxide Applications

Jean Rousset,<sup>†</sup> Edgardo Saucedo,<sup>†</sup> and Daniel Lincot<sup>\*,†,‡</sup>

*Institut de Recherche et Développement sur l'énergie photovoltaïque, UMR 7174-EDF-CNRS, 6 quai Watier, 78401 Chatou Cedex, France, and Laboratoire d'électrochimie et de chimie analytique (LECA), UMR-CNRS 7575, Ecole Nationale Supérieure de Chimie de Paris, 11 rue Pierre et Marie Curie, 75231 Paris Cedex 05, France*

Received October 10, 2008. Revised Manuscript Received December 9, 2008

A systematic study of n-type zinc oxide thin films electrodeposition in presence of chloride ions is presented in this article. The incorporation of chlorine during the growth is characterized by several techniques, and its influence on the optoelectronic properties of the films is explored. Different deposition conditions have been tested; depending on the support electrolyte nature (nitrate or perchlorate) and on the chlorine concentration introduced in the bath, a large range of carrier concentrations has been reached (from  $7.4 \times 10^{17} \text{ cm}^{-3}$  for a nitrate electrolyte without chloride ions addition to  $9 \times 10^{19} \text{ cm}^{-3}$  in perchlorate conditions with a chloride concentration of 0.1 M). This evolution of the doping concentration evaluated by Mott–Schottky measurements and confirmed by Raman spectroscopy has a great effect on the optical transmission of the films. The increase in the doping concentration tends to shift the absorption edge to higher energies and to induces the decrease of the transmission in the near-infrared range because of the free carrier absorption. We finally propose a model to explain the effective n-type doping of ZnO with Cl, based on the intrinsic and extrinsic defects of the system.

## Introduction

Zinc oxide has received much attention over the past years because of its numerous applications in such fields as piezoelectric and optoelectronic devices, chemical sensors, and photovoltaic applications.<sup>1–4</sup> A wide range of properties can be reached depending on its structure, morphology, and conductivity. Among these properties, the transparency in the visible region is assured by its wide band gap (3.3 eV for intrinsic ZnO), and its conductivity can be tuned by controlling the doping level. The choice of ZnO was primarily motivated by its non toxicity and the abundance of its components. The objective of this work is to prepare transparent and high conductive n-type zinc oxide thin films doped with chlorine, by electrodeposition. ZnO is generally a n-type semiconductor and its conductivity which strong depends on the doping level can range from insulating (intrinsic material) to high values ( $\sigma \approx 1 \times 10^4 \text{ S m}^{-1}$  for a highly doped material). The doping can be intrinsic due to an excess of zinc or a lack of oxygen or extrinsic by incorporation of different impurities in the film. Doping elements can be chosen in the III or IV columns (B, Al, Ga, In, Ge, ...) of the periodic table, in which case they substitute

Zn atoms in the lattice.<sup>5–7</sup> Alternatively elements in the VII column can substitute the oxygen in the lattice (F, Cl, I, Br).<sup>8–12</sup> Nevertheless, it is not easy to accurately control the n-type conductivity without deteriorating the optical properties, and there is a large technological interest to search new ways to obtain high conductive and transparent n-type ZnO, with high uniformity in these properties.

Moreover, up until now, doping ZnO with anions in substitution to oxygen has not been widely studied despite some promising previous reports that have identified chlorine as an effective n-type doping element.<sup>9–11</sup> On the other hand, the electrochemical method is an economical and low-temperature technique that is capable of depositing high-quality compounds on large areas.<sup>13</sup> The electrodeposition of ZnO was reported for the first time by Peulon et al.<sup>14</sup> and Izaki et al.<sup>15</sup> with dissolved oxygen and nitrate ions as electrochemical active compound, respectively. The hypothesis of the Cl doping by addition of chloride in the bath first

\* Corresponding author. E-mail: jean-externe.rousset@edf.fr. Tel: 33 1 30 87 78 45. Fax: 33 1 30 87 85 65.

<sup>†</sup> Institut de Recherche et Développement sur l'énergie photovoltaïque.

<sup>‡</sup> Laboratoire d'électrochimie et de chimie analytique (LECA).

- (1) Wacogne, B.; Roe, M. P.; Pattinson, T. A.; Pannel, C. N. *Appl. Phys. Lett.* **1995**, *67*, 1674.
- (2) Arnold, M. S.; Avouris, P.; Pan, Z. W.; Wang, Z. L. *J. Phys. Chem. B* **2003**, *107*, 659.
- (3) Stolt, L.; Hedstrom, J.; Kessler, J.; Ruckh, M.; Velthaus, K. O.; Schock, H. W. *Appl. Phys. Lett.* **1993**, *62*, 597.
- (4) Law, M.; Greene, L. E.; Johnson, J. C.; Saykally, R.; Yang, P. D. *Nat. Mater.* **2005**, *4*, 455.

- (5) Faÿ, S.; Steinhauser, J.; Oliveira, N.; Vallat-Sauvain, E.; Ballif, C. *Thin Solid Films* **2007**, *515*, 8558.
- (6) Kemell, M.; Dartigues, F.; Ritala, M.; Leskelä, M. *Thin Solid Films* **2003**, *434*, 20.
- (7) Ma, Q. B.; Ye, Z.; He, H.; Wang, J.; Zhu, L.; Zhang, Y.; Zhao, B. *J. Cryst. Growth* **2007**, *304*, 64.
- (8) Hu, J.; Gordon, R. G. *Sol. Cells* **1991**, *30*, 437.
- (9) Cui, J. B.; Soo, Y. C.; Chen, T. P.; Gibson, U. J. *J. Phys. Chem. C*, **2008**, *112*, 4475.
- (10) Tchelidze, T.; Chikoidze, E.; Gorochov, O.; Galtier, P. *Thin Solid Films* **2007**, *515*, 8744.
- (11) Chikoidze, E.; Nolan, M.; Modreanu, M.; Sallet, V.; Galtier, P. *Thin Solid Films* **2008**, *516*, 8146.
- (12) Ishizaki, H.; Imaizumi, M.; Matsuda, S.; Izaki, M.; Ito, T. *Thin solid films* **2002**, *411*, 65.
- (13) Pauporté, T.; Lincot, D. *Appl. Phys. Lett.* **1999**, *75*, 3817.
- (14) Peulon, S.; Lincot, D. *Adv. Mater.* **1996**, *8*, 166.
- (15) Izaki, M.; Omi, T.; Pattinson, T. A. *Appl. Phys. Lett.* **1996**, *68*, 2439.

proposed by Peulon et al.<sup>14</sup> have been confirmed, and recently, the effect of this element on ZnO nanowires growth was described in detail.<sup>9,16–18</sup>

This paper presents a systematic study of the electrodeposition of n-type doped ZnO thin films and describes the influence of the chloride concentration introduced in the electrolyte on the optoelectronic properties of the deposited films. The choice of this element was motivated by its high solubility in aqueous media at neutral pH.

### Experimental Section

Electrodepositions were performed at 80 °C in a conventional three-electrode cell using a VMP2 potentiostat from Princeton Applied Research and the Ec-laboratory software. The reference electrode was a saturated K<sub>2</sub>SO<sub>4</sub> mercury/mercurous sulfate electrode (MSE, + 0.65 V vs normal hydrogen electrode (NHE)), separated from the solution by an Al<sub>2</sub>O<sub>3</sub> porous junction and maintained at room temperature by a glass bridge filled with the electrolyte. A Zn foil served as the counter electrode. The films have been synthesized on F-doped SnO<sub>2</sub> coated glass with a sheet resistance of 10 Ω/sq. The substrate is chemically treated: first washed with ethanol and then with acetone (during 5 min in an ultrasonic bath) and finally dipped in a 45% HNO<sub>3</sub> solution (during 2 min in an ultrasonic bath). Two different aqueous media have been used for the electrodeposition of ZnO thin films: nitrate and perchlorate bath. The films obtained in these two different baths were compared in terms of light transmission, carrier density, composition, structure, and morphology.

The “nitrate electrolyte” was composed uniquely of dissolved zinc nitrate salt ([Zn(NO<sub>3</sub>)<sub>2</sub>] = 0.05 M). In this case, the addition of a supporting electrolyte was not necessary because of the high concentration of zinc salt introduced in the bath, moreover nitrate ions acted as oxygen precursors. Electrodepositions were also carried out in a perchlorate solution containing Zn<sup>2+</sup> ions introduced as ZnClO<sub>4</sub> ([ZnClO<sub>4</sub>] = 5 × 10<sup>-3</sup> M) and KClO<sub>4</sub> as the supporting electrolyte (5 × 10<sup>-2</sup> M), the bath was in this case saturated with oxygen gas. To show the effect of the dissolution of chloride ions in the bath on the material properties, we have progressively added Cl<sup>-</sup> ions from KCl salts to the solution. The Cl<sup>-</sup> concentration ranged from 0 to 0.1 M. Deposition experiments have been performed under potential control (-1.4 V/MSE). In nitrate conditions an electrochemical pretreatment was carried out by applying a current density of 4 mA cm<sup>-2</sup> during 15 s in order to improve the film quality. This treatment has been shown to enhance the number of nuclei on the substrate surface, thus allowing the synthesis of dense and highly transparent ZnO films.<sup>19</sup> Electrodepositions were carried out during approximately one hour corresponding to thicknesses ranging from 0.6 to 2.2 μm.

The morphology and composition of the films was studied using a scanning electron microscope (LEICA S440), coupled to an EDX analyzer. Raman microprobe measurements were made using a HR800-UV Horiba-Jobin Yvon spectrometer coupled with an Olympus metallographic microscope. The spectra measured on the samples were obtained using as excitation the green line of an Ar<sup>+</sup> laser (λ = 514 nm) under unpolarized conditions. The spectra were fitted using the LabSpec software defining the peaks as Gaussian-Lorentzian.

The electrolyte for processing the Mott-Schottky measurements is a phosphate buffer solution (pH 7) in which 0.1 M of KClO<sub>4</sub> is added. The contact to the F-doped SnO<sub>2</sub> substrate is made after the dissolution of a part of the ZnO layer in 0.1 M HCl acidic solution. A surface area of 0.07 cm<sup>2</sup> is isolated on ZnO films and exposed to the electrolyte. The potential scan is carried out from -1.6 V/MSE to 1.2 V/MSE using a ±20 mV amplitude signal at 10 kHz. The weak current density observed during the Mott-Schottky measurement (<50 μA cm<sup>-2</sup>) allows us to consider that the sample is not altered by this experiment.

The optical transmission spectra were measured at room temperature using a Perkin-Elmer lambda 900 spectrometer.

### Results and Discussion

To study the growth kinetic of the films, we calculated the growth rate from the film thicknesses observed on the SEM images (see Figure 1). Their comparison with those calculated from the consumed charge during the deposition shows that the faradic efficiency is higher than 90% for each of the tested conditions. In the perchlorate electrolyte the growth rate is relatively low (0.45–0.6 μm h<sup>-1</sup>) with respect to that obtained in the nitrate one (2.5 μm h<sup>-1</sup>) and remains reasonably constant for KCl concentrations ranging from 0 to 0.1 M. It is observed that the deposition mechanism of ZnO is strongly dependent on the nature of the aqueous media used. In the perchlorate electrolyte, the chronoamperometric curve reaches a minimum value and suggests a three-dimensional electrocrystallization (not shown).<sup>20</sup> In such a case, isolated nuclei grow on the electrode surface increasing the active surface, until they come into contact with their near neighbors nuclei. This type of growth first causes the decrease, then the increase and finally the stabilization of the total current leading to the formation of large grains. In this electrolyte condition, the deposition process is partially limited by the oxygen diffusion at the working electrode surface, and thus the growth rate is a function of its concentration in the bath and of the stirring conditions. The amount of Zn introduced in the electrolyte only weakly influences the current density weakly.

In contrast, when a nitrate bath is used, the deposition process has a kinetic limitation. The growth rate is affected by the zinc concentration, the metal ions that are adsorbed on the electrode surface catalyze the nitrate reduction and then enhance the growth rate.<sup>21</sup> The higher concentration of Zn(NO<sub>3</sub>)<sub>2</sub> introduced in the nitrate electrolyte compared to the saturation concentration of oxygen (0.8 × 10<sup>-3</sup> M at 80 °C) in water explains the growth rate variation between the two electrolytes.

**Morphology and Composition.** The morphologies of the films obtained in the nitrate electrolyte and the perchlorate with 0.03 M chloride ions are shown in Figure 1. The films deposited from the perchlorate electrolyte for all tested chloride concentrations present a dense morphology and are composed of large hexagonal grains perpendicular to the substrate surface. The increase of the chloride amount in the bath does not seem to have any influence nor in the global

(16) Peulon, S.; Lincot, D. *J. Electrochem. Soc.* **1998**, *145*, 864.

(17) Elias, J.; Tena Zaera, R.; Levy-Clément, C. *J. Phys. Chem. C* **2008**, *112*, 5736.

(18) Tena Zaera, R.; Elias, J.; Wang, G.; Levy-Clément, C. *J. Phys. Chem. C* **2007**, *111*, 16706.

(19) Canava, B.; Lincot, D. *J. Appl. Electrochem.* **2000**, *30*, 711.

(20) Pauporté, T.; Lincot, D. *Electrochim. Acta* **2000**, *45*, 3345.

(21) Yoshida, T.; Kamotsu, D.; Shimokawa, N.; Minoura, H. *Thin Solid Films* **2004**, *451*, 166.



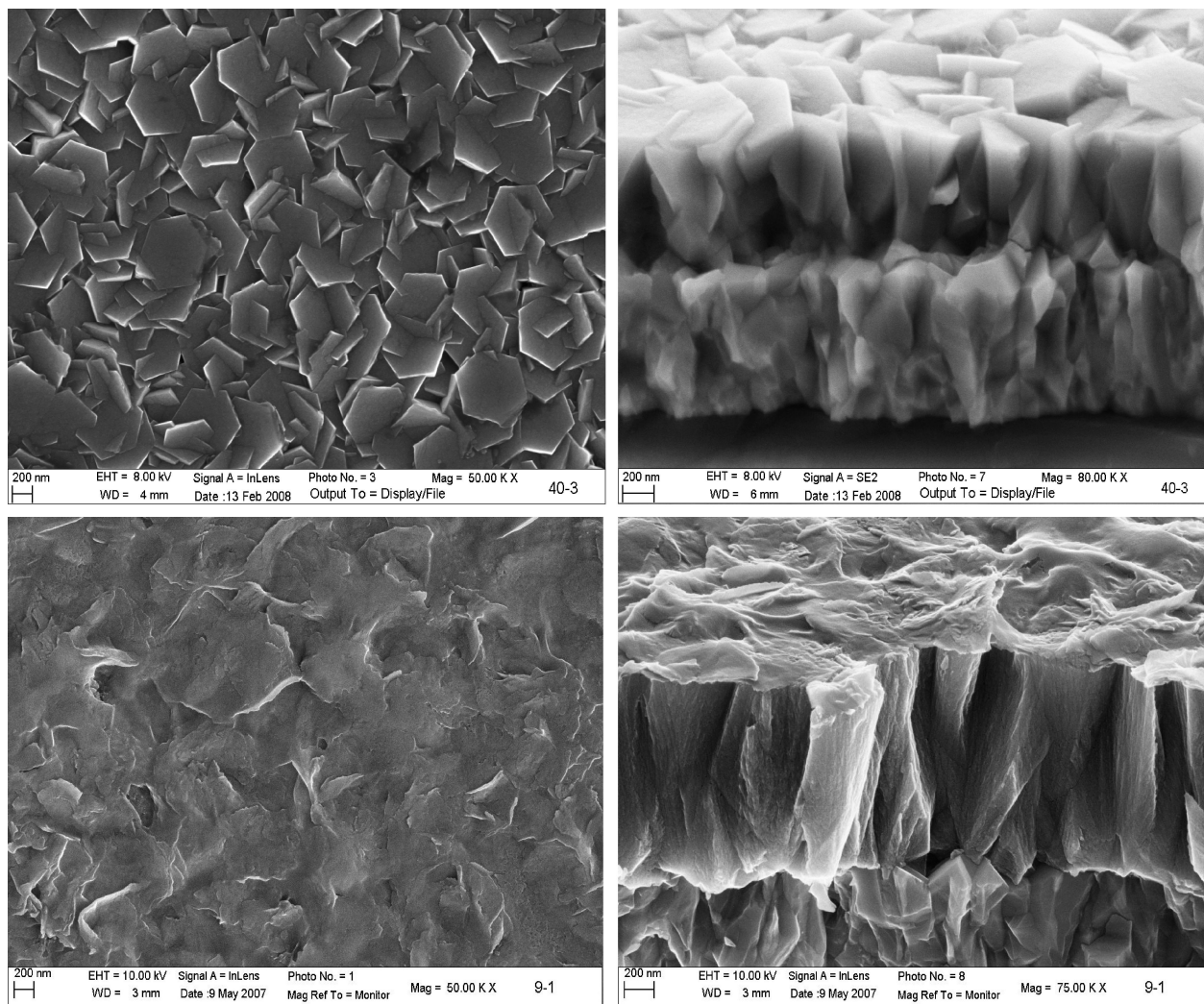


**Figure 1.** Morphology of films obtained in a perchlorate electrolyte containing 0.03 M of chlorine ions (top images) and in a nitrate electrolyte (bottom images).

morphology, neither in the crystallites orientation. Conversely, the film synthesized in the nitrate bath shows less-defined hexagonal structures and its surface is smoother than those of “the perchlorate films”. The composition is analyzed by EDX measurements. The intensity of the chloride signal (peak at 2.63 keV) is enhanced as a function of the KCl concentration (Figure 2a). The Cl atomic concentration ranges from 0.9% for a pure perchlorate electrolyte to 3% for a chloride concentration of 0.1 M (Figure 2b). The detection of chlorine in the material even if no KCl is added to the electrolyte shows that perchlorate ions can act as a source of chloride. But this effect is much weaker than that of adding chloride ions in the bath. The atomic concentration of chlorine in the film first increases sharply as a function of chloride concentration before reaching a value (close to atomic ratio Cl/Zn = 3% for  $[\text{Cl}^-] = 0.03 \text{ M}$ ) corresponding to a saturation phenomenon. The samples were cleaned with deionized water directly after the growth in order to eliminate eventual chloride salt traces on film surfaces. So the EDX measurements are expected to show the incorporation of chlorine atoms into the ZnO bulk.

**Raman Spectroscopy.** The Raman spectra of the different studied samples are shown in Figure 3. Among others, four important features are observed in the studied region at

frequency close to 285, 395 (its position strongly depends on the composition), 439, and 465  $\text{cm}^{-1}$ . The only one that can be unambiguously assigned to ZnO is the mode at 439  $\text{cm}^{-1}$ , which corresponds to the  $E_2$  vibration of the wurtzite phase.<sup>22–26</sup> The position of this peak seems to not depend on the KCl concentration, ranging its frequency between 439 and 440  $\text{cm}^{-1}$ . This value is lightly blue-shifted with respect to that of bulk ZnO, suggesting that the films are under compressive residual stresses. Although no relevant change is observed in the Raman shift, it is observed in Figure 3 that this peak is wider and lower with the increasing Cl concentration and, at the same time, the other three peaks appear and start to be more and more intense. Among these peaks, two of them have a similar behavior, whereas the other behaves very differently.

- (22) Bundesmann, C.; Ashkenov, N.; Shubert, M.; Spemann, D.; Butz, T.; Kaidashev, E. M.; Lorenz, M.; Grundmann, M. *Appl. Phys. Lett.* **2003**, *83*, 1974.
- (23) Huang, T.; Zhou, S.; Teng, H.; Lin, H.; Wang, J.; Hang, P.; Zhang, R. *J. Cryst. Growth* **2008**, *310*, 3144.
- (24) Kumar Tripathy, S.; Sahoo, T.; Lee, I.; Yu, Y. *Mater. Lett.* **2007**, *61*, 4690.
- (25) Calleja, J. M.; Cardona, M. *Phys. Rev. B* **1977**, *16*, 3753.
- (26) Kaschner, A.; Haboeck, U.; Strassburg, M.; Kaczmarczyk, G.; Hoffmann, A.; Thomsen, C.; Zeuner, A.; Alves, H. R.; Hofmann, D. M.; Meyer, B. K. *Appl. Phys. Lett.* **2002**, *80*, 1909.

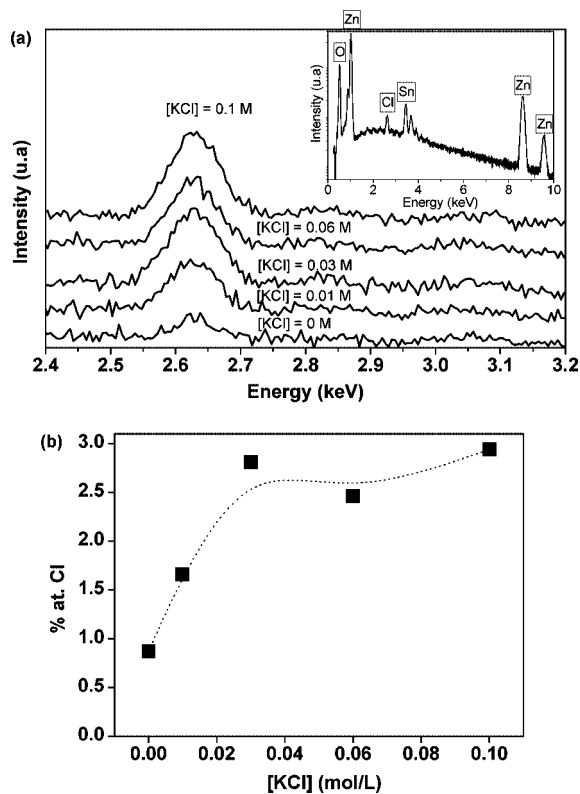


**Figure 2.** (a) Evolution of the chlorine peak with the electrolyte composition; inset: EDX spectrum carried out on a film deposited in a perchlorate electrolyte containing 0.03 M of chlorine ions (logarithmic scale). (b) Evolution of the Cl atomic concentration as a function of the KCl concentration ranging from 0 to 0.1 M.

The peaks at 284 and 465  $\text{cm}^{-1}$  seem to not shift with the KCl concentration but in contrast, their intensity significantly increases. Recent work has shown that the mode at 284  $\text{cm}^{-1}$  originates from host lattice defects<sup>22</sup> and has been obtained for ZnO samples doped with N, Fe, Sb, Al and Ga.<sup>22–26</sup> We observe this mode also for Cl doped ZnO although with a blue-shift with respect to the values presented in the literature. This is a confirmation of the origin of this mode, which presumably is related to distortions introduced in the lattice by the incorporation of Cl. In such a case, indirectly Cl leads to the formation of an intrinsic defect that can play a role on the electrical properties of the samples. The mode at 465  $\text{cm}^{-1}$  shows a similar behavior to that at 284  $\text{cm}^{-1}$ , suggesting that both can be related, but this point need a deeper study for further confirmation.

Conversely, the additional mode close to 400  $\text{cm}^{-1}$  behaves completely different. A strong red-shift from 425  $\text{cm}^{-1}$  for [KCl] = 0 M to 394  $\text{cm}^{-1}$  for [KCl] = 0.1 M is observed, together with the increase of its intensity. This could be a direct evidence that this additional mode originates from the doping being useful as Cl incorporation marks. Its intensity does not increase linearly with the KCl concentration (Figure 3b), but this result is logical if we take into account that the Cl incorporation is also not linear with the KCl concentration. In fact, the fundamental Zn–Cl vibration mode (stretching mode), can vary their frequency from 400 to 300  $\text{cm}^{-1}$  strongly depending on their environment.<sup>27,28</sup> On the basis of these results, we propose that this mode is due to the Zn–Cl stretching vibration, implying the formation of the extrinsic defect Cl<sub>O</sub>, i.e., the chlorine atoms act as O substitutes.

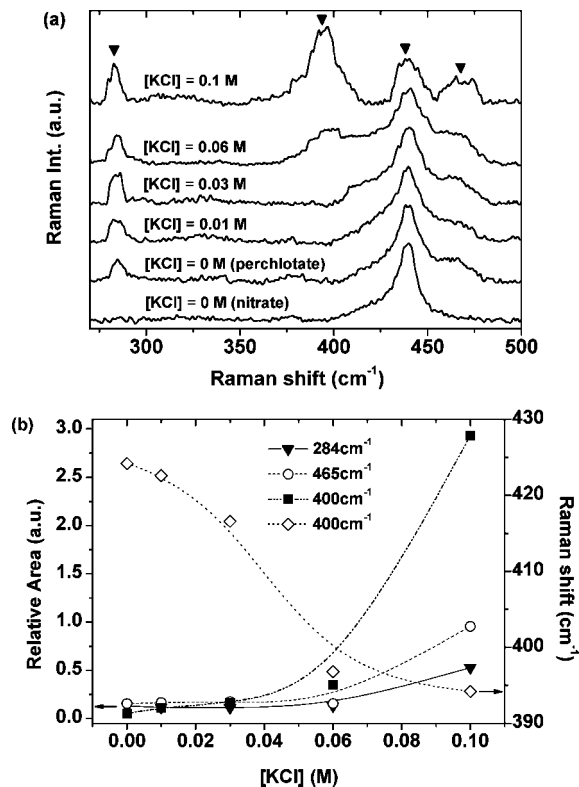


**Figure 3.** (a) Raman spectra obtained on films deposited in nitrate and perchlorate electrolytes ( $0 \text{ M} < [\text{KCl}] < 0.1 \text{ M}$ ). (b) Evolution of the relative area of Raman modes with respect to the  $E_2$  vibration mode of wurtzite ZnO (240  $\text{cm}^{-1}$ ) and evolution of the Raman shift of the mode assigned to Cl incorporation (which ranges from 430 to 395  $\text{cm}^{-1}$ ) as a function of the KCl concentration.

Supported by the following electrical and optical characterization, we will try to confirm the supposed origin of the extrinsic defect.

**Carrier Concentration.** Some authors demonstrated that ZnO films can be doped with chlorine atoms.<sup>9–11</sup> This element can theoretically be inserted in the ZnO lattice in substitution to oxygen introducing an extrinsic donor energy level. Mott–Schottky measurements have been carried out in order to evaluate the impact of electrolyte nature on the electrical properties of the deposited material. This method is based on the Schottky barrier formation between the semiconductor material and the electrolyte.<sup>29–31</sup> If the electrolyte is concentrated enough, the voltage drop due to the inverse polarization and the Schottky barrier are completely distributed in the semiconductor material. It causes the creation of a depletion zone that can be characterized by a capacitance measurement. If the system obeys Mott–Schottky behavior, the evolution of  $1/C^2$  is a linear function of the applied potential. The sign and the value of its slope is representative of the doping type and of the carrier

- (27) Tenenbaum, E. D.; Flory, M. A.; Pulliam, R. L.; Ziurys, L. M. *J. Mol. Spectrosc.* **2007**, *244*, 153.  
 (28) Tepavitcharova, S.; Havlíček, D.; Nemeč, I.; Vojtíšek, P.; Rabadjeva, D.; Ploček, J. *J. Mol. Struct.* **2008**, in press.  
 (29) Cardon, F.; Gomes, W. P. *J. Phys. D: Appl. Phys.* **1978**, *11*, L63.  
 (30) Windisch, C. F.; Exarhos, G. J. *J. Vac. Sc. Technol.* **2000**, *18* (4), 1677.  
 (31) Mora-Sero, I.; Fabregat-Santiago, F.; Denier, B.; Bisquert, J.; Tena-Zaera, R.; Elias, J.; Lévy-Clément, C. *Appl. Phys. Lett.* **2006**, *89*, 203117.

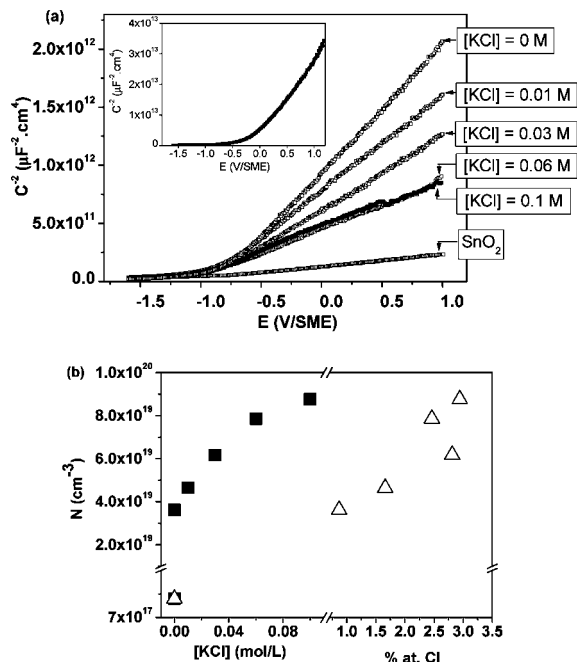


**Figure 4.** (a) Mott–Schottky measurements on the films deposited in perchlorate electrolyte containing different chlorine concentrations; inset: Mott–Schottky measurement on the film deposited in the nitrate electrolyte. (b) Carrier concentration as function of the chlorine concentration and as a function of the atomic ratio Zn/Cl obtained by EDX analyses.

concentration ( $N$ ), respectively. This latter can be determined from the slope of this curve, using the equation

$$\frac{1}{C^2} = \left( \frac{2}{e\epsilon_0\epsilon_r N_D A^2} \right) \left( V - V_{FB} - \frac{kT}{e} \right) \quad (1)$$

Where  $C$  is the capacitance of the space charge region of the film at potential  $V$ ,  $V_{FB}$  is the flatband potential,  $N_D$  is the free carrier concentration of the semiconductor,  $A$  is the delimited area in contact with the electrolyte, the assumption of a perfectly smooth surface is made,  $\epsilon_0$  is the permittivity of the free space, and  $\epsilon_r$  the relative dielectric constant taken as the typical value for bulk ZnO (8.0). The Mott–Schottky plots obtained on the films deposited in nitrate and perchlorate electrolytes are shown in Figure 4a. They are linear as expected, and the decrease of the measured capacity (increase in  $1/C^2$ ) when the applied potential is shifted to cathodic values is the mark of a n-type semiconductor. Moreover great differences can be noticed according to the nature of the electrolyte. The evolution of  $1/C^2$  becomes progressively smoother when chloride ions are added to the electrolyte. This phenomenon is typical when the carrier concentration increases. The values extracted from Mott–Schottky plots are presented as a function of the chloride concentration in the bath and as a function of the atomic ratio Cl/Zn (Figure 4b). The carrier concentration increases by almost 2 orders of magnitude when the material is synthesized in the pure perchlorate electrolyte ( $3.7 \times 10^{19} \text{ cm}^{-3}$ ) as compared to the nitrate condition ( $7.4 \times 10^{17} \text{ cm}^{-3}$ ). The carrier concentration is also enhanced by the increase of the chloride quantity introduced in the bath, and ranges from  $3.7 \times 10^{19} \text{ cm}^{-3}$  for  $[\text{Cl}^-] = 0 \text{ M}$  (“pure” perchlorate conditions) to  $9 \times 10^{19} \text{ cm}^{-3}$  for  $[\text{Cl}^-] = 0.1 \text{ M}$ . This latter value seems to be close to the maximum reachable carrier concentration in these conditions. Indeed, the curve  $N = f([\text{KCl}])$  tends toward

a saturation value, and the chloride concentration can not be indefinitely increased. The flat band potential is shifted to more cathodic values when the chlorine concentration is increased in the electrolyte (not shown), and this phenomenon is also related to the evolution of the free carrier concentration in the material.

The maximum carrier concentration ( $9 \times 10^{19} \text{ cm}^{-3}$ ) detected by Mott–Schottky measurements corresponds to a chlorine atomic concentration of 0.4% in the film (considering an atom density of  $2 \times 10^{22} \text{ cm}^{-3}$ ). This value stays much lower than the chlorine rate detected by EDX, this variation can be explain by the formation of zinc salts in the material as  $\text{ZnCl}_2$ , self-compensation of the doping, or by formation of neutral Cl related defects.

Then, the n-type doping of ZnO:Cl can be explained by intrinsic, extrinsic or more probably by both mechanisms. The formation of the intrinsic defect observed at  $284 \text{ cm}^{-1}$  by Raman spectroscopy (see Figure 3a) is related to a compression of the bonds responsible of this mode. Although there are no direct evidence, on the basis of earlier studies, we propose that this intrinsic defect arise from the approach of two O atoms and the formation of a like-dimer of these atoms.<sup>32</sup> When Cl occupy O sites, they act as donor defect ( $\text{Cl}_O^{0/+}$ ), forcing the elongation of the Cl–Zn bond. At the same time, two O near neighbor atoms of Zn are forced to approach forming the VI–VI like-dimer. This type of intrinsic defect introduces deep donor levels<sup>26</sup> and then are not able to explain the effective n-type doping of the samples. Nevertheless, the extrinsic defect already observed by Raman spectroscopy ( $\text{Cl}_O^{0/+}$ ) has all the characteristics allowing to explain the electrical properties of the samples: it is a donor defect and the halogens introduce shallow levels in II–VI semiconductors, being the most probably extrinsic defect able to explain the increase of the doping level with the Cl concentration.

**Optical Properties.** The optical properties of the deposited films have been explored by optical transmission and the corresponding spectra are shown in panels a and b in Figure 5. The total transmission of the glass/SnO<sub>2</sub>/ZnO system is represented with air (Figure 5a) or glass/SnO<sub>2</sub> as references (Figure 5b). The electrodeposited films present, for each set of deposition conditions, a high transmission in the visible wavelength range and a sharp absorption onset. Two major evolutions can be noticed depending on the nature of the bath. The first visible in the inset of the Figure 5b ( $(\alpha h\nu)^2 = f(h\nu)$ ) concerns the position of the absorption onset, which shifts to shorter wavelengths (higher energies) with the increase in the carrier concentrations in the film. The variation in  $(\alpha h\nu)^2$  is linear as a function of  $h\nu$  in the wavelength range of the absorption edge. Its shape, which is a trademark of a direct band gap material, allows us to determine the optical band gap by extrapolation. Figure 6 shows that the optical band gap is closely connected to the growth conditions. Nitrate bath deposition yields a bandgap of 3.3 eV, close to that of bulk intrinsic ZnO. The carrier concentration drops when the electrolyte nature is changed ( $E_g = 3.5 \text{ eV}$  for the pure perchlorate electrolyte). Moreover,  $E_g$  increases at first sharply with the chloride concentration and finally



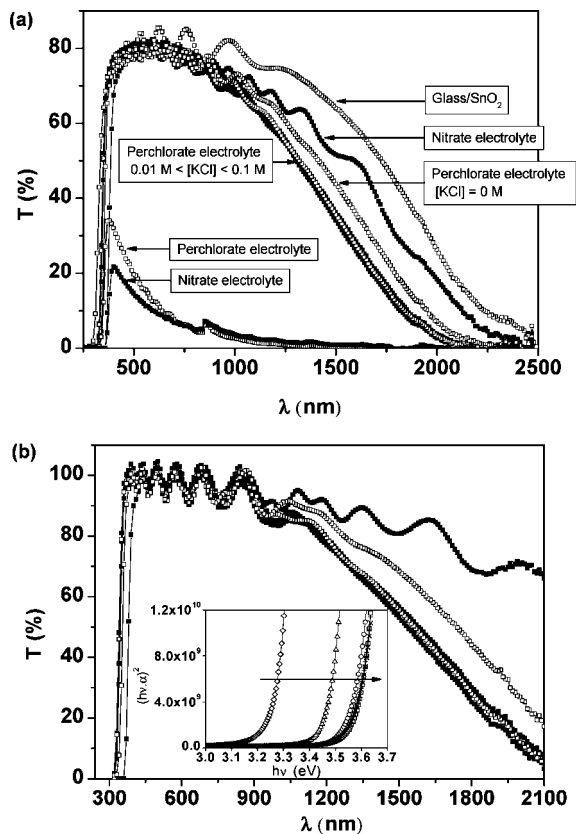


**Figure 5.** (a) Total transmission obtained on films deposited in nitrate and perchlorate electrolytes (0 M < [KCl] < 0.1 M). Air taken as reference. Diffuse transmission obtained on films deposited in nitrate and pure perchlorate electrolytes. Air taken as reference. (b) Total transmission obtained on films deposited in nitrate and perchlorate electrolytes (0 M < [KCl] < 0.1 M). Glass/SnO<sub>2</sub> taken as reference; inset:  $(\alpha h\nu)^2 = f(h\nu)$  representation from the transmission data obtained on films deposited in nitrate and perchlorate electrolytes (◇, nitrate electrolyte; △, pure perchlorate electrolyte; ○, [KCl] = 0.01 M; ×, [KCl] = 0.03 M; □, [KCl] = 0.06 M; +, [KCl] = 0.1 M).

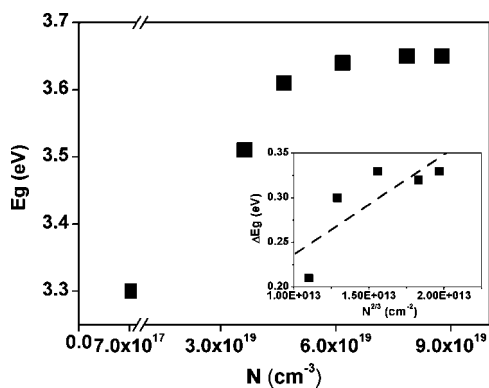


**Figure 6.** Band gap value as a function of the carrier concentration; inset: representation of the band gap shift as a function of  $N^{2/3}$ .

stabilizes around 3.65 eV. This  $E_g$  shift could be considered as further evidence of chlorine incorporation into the material. This phenomenon can be attributed to the so-called Moss–Burstein effect.<sup>33,34</sup> It occurs when carrier concentrations are such that electrons partly fill the conduction band. As a result, optical absorption measurements overestimated

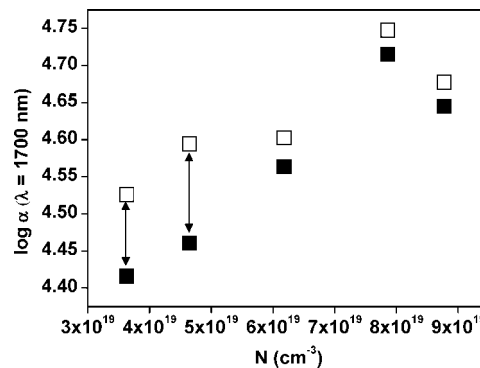


**Figure 7.** Absorption coefficient as a function of the carrier concentration measured just after the growth (□) and after a 48 h storage in air (■).

the band gap due to the additional energy required to excite electrons from the top of the valence band to the Fermi level within the conduction band (degenerated semiconductor). The variation in  $E_g$  with  $N^{2/3}$ , characteristic of this effect, is presented in Figure 6 (inset) for the five samples with highest doping concentrations synthesized in the perchlorate electrolyte. The linear coefficient ( $11 \times 10^{-15} \text{ cm}^{-3}$ ) obtained is close to that calculated ( $9 \times 10^{-15} \text{ cm}^{-3}$ ) from the theory and validates the Mott–Schottky measurements of the carrier concentration.

The second evolution of the transmission curves with the change of the bath composition is located in the near-infrared part of the spectra. While the transmission remains quite constant in the wavelengths ranging from 400 to 900 nm, it clearly depends on the bath conditions (and then on the doping) for wavelengths superior to 900 nm. This effect can be related to the free carrier absorption and has been quantified by considering the absorption coefficient at  $\lambda = 1700$  nm.<sup>5</sup> As expected from the transmission spectra, the absorption coefficient increases with the carrier concentration (Figure 6). Moreover for a given carrier concentration, the absorption coefficient decreases as a function of the storage time of the samples grown in the perchlorate electrolytes without adding chlorine ions and those containing 0.01 M of Cl<sup>-</sup>. In contrast, for the other conditions tested, the absorption coefficient remains quite constant with time. This effect can be explained by considering two different kinds of doping which can be effective in the case of electrodeposited ZnO in the presence of chloride ions. The carrier concentration can be enhanced by intrinsic doping or by extrinsic doping (for instance, the incorporation of chlorine impurities which is the topic of this study). The first has been shown to be unstable over long storage time by the plot on Mott–Schottky curves carried out on samples grown in a nitrate electrolyte (not shown). The doping that is expected to be intrinsic in this deposition conditions could be lowered in contact with the oxygen from the atmosphere. Thus in the case of samples grown in the perchlorate electrolyte, absorption coefficient’s decrease with time could be related to the intrinsic part of the doping in the material. The stability of the carrier concentration for the samples grown in electrolyte with highest chlorine concentrations can be considered as an indirect mark of extrinsic ZnO doping.

Figure 5a compares the diffuse transmission (with air as reference) of the film deposited in the nitrate electrolyte and

(33) Martinez, A. I.; Acosta, D. R. *Thin Solid Films* **2005**, *483*, 107.  
 (34) Lee, H. W.; Lau, S. P.; Wang, Y. G.; Tse, K. Y.; Hng, H. H.; Tay, B. K. *J. Cryst. Growth* **2004**, *268*, 596.

in the pure perchlorate electrolyte. These curves show that the diffusive properties of the films are higher in the short wavelengths range and decreases when the incident light energy is shifted to lower energies. The diffusion phenomenon is due to the film surface roughness. So the smoother surface obtained in the nitrate electrolyte makes the film less diffusive than that deposited in the perchlorate one. This can be related to the electrochemical pre treatment which leads to a deposition process close to a two-dimensional growth. The grains are smaller than that obtained with a three-dimensional growth and smooth the sample surface.

### Conclusion

This paper presents a systematic study dealing with the electrodeposition of dense ZnO layers containing chlorine impurities for transparent conductive oxide applications. The effect of the electrolyte nature (nitrate or perchlorate) and the addition of chloride ions in the bath on the morphology, the structure, the carrier concentration and the optical properties of the ZnO layers have been investigated. Compact films with high transmission in the visible wavelengths range and containing high carrier density (up to  $9 \times 10^{19} \text{ cm}^{-3}$ ) have been obtained. Compositional analysis, optical and Mott–Schottky measurements allowed to demonstrate that

the doping is extrinsic and achieved by incorporation of chlorine into the layer. Using Raman spectroscopy an intrinsic defect is detected and assigned to O like-dimers which introduce a deep donor level, and do not affect significantly the electrical properties. Also, an active Raman mode is observed at  $400 \text{ cm}^{-1}$  approximately, with a position and an intensity which strongly depend on the Cl concentration. We propose a defect model in which ( $\text{Cl}_\text{O}^{0/+}$ ) can explain all the properties of ZnO:Cl presented in this study. On the other hand, electrochemical deposition in electrolytes containing chloride ions appears to be a very interesting way to synthesize transparent conductive oxides because this technique is easy to carry out and economical. The choice of a chlorine species is also a promising because of its behavior in a aqueous medium. In contrast to classical doping species like indium the solubility of chlorine ions is high at the pH used during the synthesis (close to neutral pH). This work opens the perspectives of using electrodeposited ZnO:Cl layers as an alternative to other TCO's for numerous optoelectronic applications.

**Acknowledgment.** We thank European integrated ATHLET project, which supports this study.

CM802765C